Research Square

Preprints are preliminary reports that have not undergone peer review.
They should not be considered conclusive, used to inform clinical practice,
or referenced by the media as validated information.

mPTP sensitization and calcium channel remodeling: an adaptive response in carboplatin-resistant ovarian cancer cells

Olivier Romito

olivierromito@gmail.com

Inserm UMR 1069, Niche Nutrition Cancer et Métabolisme Oxydatif, Université de Tours

Ophélie Champion

Inserm UMR 1069, Niche Nutrition Cancer et Métabolisme Oxydatif, Université de Tours

Aude Lemettre

Inserm UMR 1069, Niche Nutrition Cancer et Métabolisme Oxydatif, Université de Tours

Mohamed Trebak

University of Pittsburgh

Caroline Goupille

Inserm UMR 1069, Niche Nutrition Cancer et Métabolisme Oxydatif, Université de Tours

Marie Potier-Cartereau

Inserm UMR 1069, Niche Nutrition Cancer et Métabolisme Oxydatif, Université de Tours

Research Article

Keywords: morusin, mPTP, Ca2+ signaling, SOCE, chemoresistance

Posted Date: November 1st, 2026

DOI: https://doi.org/10.21203/rs.3.rs-11125252/v1

License: This work is licensed under a Creative Commons Attribution 4.0 International License.
Read Full License

Additional Declarations: Competing interest reported. Mohamed Trebak is a paid consultant of Seeker Biologics Inc.

Abstract

Acquired resistance to chemotherapy represents a major obstacle to the long-term efficacy of treatment in ovarian cancer. In this study, we investigated the impact of acquired resistance to Taxol® and carboplatin on mitochondrial permeability transition pore (mPTP) sensitivity and Ca^{2+} homeostasis in high-grade serous ovarian cancer (HGSOC) cells. Taxol®-resistant cells exhibited no detectable alterations in mPTP sensitivity or Ca^{2+} signaling. In contrast, carboplatin-resistant cells displayed increased mPTP sensitivity accompanied by a marked reduction in endoplasmic reticulum Ca^{2+} release, store-operated Ca^{2+} entry, constitutive Ca^{2+} entry, and mitochondrial Ca^{2+} uptake. These alterations were associated with reduced mRNA expression of Orai1, STIM1, KCNN2, KCNN3, and MCU. Consistent with these findings, low tumoral expression of *ORAI1* was associated with disease progression and an unfavorable response to platinum-based treatment in patients with ovarian cancer. Short-term exposure to carboplatin was sufficient to sensitize the mPTP in non-cancerous HEK-293 cells, suggesting that this effect results from a direct action of the drug rather than from an adaptive phenotype acquired through prolonged drug selection. Pharmacological attenuation of carboplatin-induced mPTP sensitization using morusin was associated with increased basal mitochondrial Ca^{2+} and carboplatin-induced cytotoxicity. Taken together, our data support a two-steps model of cellular adaptation to carboplatin. The initial response involves increased mPTP sensitivity, which may promote the release of excess mitochondrial Ca^{2+}. This is followed by a broader downregulation of Ca^{2+} entry pathways, thereby limiting the Ca^{2+} load reaching an intrinsically sensitized mPTP. Further studies are required to elucidate the molecular mechanisms linking these adaptive responses.

1. Introduction

Ovarian cancer remains the deadliest gynecological malignancy, (Sung et al., 2021; Zheng, 2017) largely due to the emergence of resistance to platinum and taxane-based chemotherapy, which are used as conventional first-line treatment (Dalton et al., 1995; Ozols et al., 2003; Zheng, 2017). Although most patients initially respond to therapy, relapse is common and is frequently accompanied by the development of chemoresistance (Siddik, 2003), severely limiting treatment options (Chatelut, 2011). Elucidating the cellular adaptations that support the acquisition of resistance is therefore critical for the development of more effective therapeutic strategies. Remodeling of Ca^{2+} signaling has emerged as a recurrent feature of chemoresistant cancers (Al-Taweel et al., 2014; Flourakis et al., 2010; Kondratska et al., 2014; Romito et al., 2022). Enhanced Ca^{2+} influx through store-operated Ca^{2+} entry (SOCE) and constitutive Ca^{2+} entry (CCE) has been linked to tumor progression and resistance to therapy in several cancer types, including ovarian, pancreatic and lung cancer (Hasna et al., 2018; Huang et al., 2020; Kondratska et al., 2014; Liu et al., 2018; Mohr et al., 2019; Schmidt et al., 2014; Tang et al., 2017). Conversely, impaired ER-to-mitochondria Ca^{2+} transfer has also been associated with resistance to platinum-based chemotherapy, (Al-Taweel et al., 2014; Arbel and Shoshan-Barmatz, 2010; Marchi and Pinton, 2013; Romito et al., 2022; Tajeddine et al., 2008; Xu et al., 2015) highlighting the complexity and context-dependency of Ca^{2+} signaling adaptations during cancer progression.

At the center of these processes, mitochondria integrate cytosolic and organellar Ca^{2+} signals to regulate cellular bioenergetics and survival. Mitochondrial Ca^{2+} uptake, primarily mediated by the mitochondrial Ca^{2+} uniporter (MCU) (Bravo-Sagua et al., 2017; Marchi et al., 2018), critically influences the sensitivity of the mitochondrial permeability transition pore (mPTP) (Zhao et al., 2022), a key regulator of cell death (Robichaux et al., 2023). While sustained, high-conductance opening of the mPTP triggers mitochondrial dysfunction and cell death (Bernardi et al., 2023; Eubler et al., 2026; O. Liu et al., 2025), transient low-conductance "flickering" events have been proposed to participate in mitochondrial Ca^{2+} homeostasis by relieving excessive matrix Ca^{2+} accumulation (Agarwal et al., 2017; Bernardi et al., 2023; Bernardi and Von Stockum, 2012; Protasoni et al., 2024). Whether chemotherapy-induced remodeling of Ca^{2+} signaling pathways contributes to the regulation of mPTP sensitivity during the acquisition of chemoresistance remains unknown.

In this study, we used carboplatin- and Taxol®-resistant sublines of the high-grade serous ovarian cancer cell line COV504 to investigate the relationship between Ca^{2+} signaling remodeling and mPTP regulation in distinct resistance phenotypes. We show that carboplatin resistance is associated with enhanced mPTP sensitivity together with a coordinated reduction in Ca^{2+} entry and mitochondrial Ca^{2+} uptake pathways, whereas Taxol® resistance does not significantly alter either process. We further demonstrate that carboplatin sensitizes the mPTP, suggesting that this response precedes and potentially drives subsequent remodeling of the cellular Ca^{2+} machinery. Finally, pharmacological attenuation of mPTP sensitization by morusin increases mitochondrial Ca^{2+} accumulation and enhances carboplatin-induced cytotoxicity. Collectively, our findings support a model in which mPTP sensitization constitutes an early adaptive response to carboplatin exposure that is subsequently reinforced by downregulation of Ca^{2+} influx pathways to limit mitochondrial Ca^{2+} overload and promote cell survival.

2. Materials and methods

2.1. Cell culture and resistant cell selection

Human high-grade serous ovarian cancer cells (COV504, RRID: CVCL_2424) were maintained in Dulbecco's Modified Eagle Medium (DMEM; Gibco, Illkirch, France) supplemented with 10% fetal bovine serum (FBS; HyClone, Lonza Bioscience, Illkirch, France) at 37°C in a humidified atmosphere containing 5% CO_2. A carboplatin-resistant subline (COV504 CP) and a Taxol®-resistant subline (COV504 TX) were generated by continuous exposure to carboplatin (10 µM; CHRU Bretonneau, Tours, France) or Taxol®, as described before (Romito et al., 2024). Subsequently, COV504 CP and COV504 TX cells were cultured in standard DMEM supplemented with 10% FBS supplemented respectively with 10 µM carboplatin or 5 nM of Taxol® to maintain the chemoresistant phenotype. HEK-293 (ATCC: CRL-1573™) were cultivated in DMEM media (Gibco, Illkirch, France), supplemented with 10% fetal bovine serum (FBS; HyClone, Lonza Bioscience, Illkirch, France) at 37°C in a humidified atmosphere containing 5% CO_2.

2.2. Survival assay

Cell viability was assessed using the tetrazolium salt reduction (MTT) assay as described previously (Romito et al., 2024). Cells were seeded in 48-well plates (10,000 cells per well) and were treated with increasing concentrations of carboplatin or Taxol® diluted in complete medium containing 10% FBS. Treatments were performed at 24h and 96h after seeding. At 7 days, survival was assessed by measuring MTT absorbance at 570 nm. Results are expressed as the percentage of cell viability relative to the untreated control condition.

2.3. Solutions for calcium recordings

Ca^{2+}-free PSS contained NaCl (140 mM), KCl (4.7 mM), MgCl2 (13 mM), HEPES (10 mM) and EGTA (1 mM). For cytosolic and mitochondrial Ca^{2+} measurements, PSS was supplemented with 2 mM CaCl2 (PSS 2Ca), and for mPTP sensitivity assays with 0.5 mM CaCl2 (PSS 0.5Ca). All solutions were adjusted to pH 7.4 with NaOH.

2.4. Store-Operated Ca^{2+} Entry measurement

Cytosolic Ca^{2+} levels were measured at 37°C using the Fura-2-AM ratiometric fluorescence dye (F340/F380) (Invitrogen™, Illkirch, France) on a FlexStation3 plate reader (Molecular Devices) as described before (Romito et al., 2024). Endoplasmic reticulum Ca^{2+} store depletion was induced by the addition of thapsigargin (4 µM; Invitrogen™, Illkirch, France) or lysophosphatidic acid (10 µM; 0.4% BSA, Aventi Polar Lipids, Alabaster, AL, USA), followed by the re-introduction of extracellular Ca^{2+} (5 mM $CaCl_2$) to assess SOCE. The maximal fluorescence ratio obtained after Ca^{2+} store depletion or Ca^{2+} re-introduction was compared to baseline (R_0) to calculate the amplitude (Rmax – R_0), reflecting intracellular Ca^{2+} release and extracellular Ca^{2+} entry.

2.5. Constitutive Ca^{2+} entry

Constitutive Ca^{2+} entry was assessed using the Mn^{2+} quench assay, based on the ability of Mn^{2+} to enter cells through Ca^{2+}-permeable channels and quench Fura-2 fluorescence at its isosbestic excitation wavelength (360 nm). Cells were loaded with Fura-2-AM, and media was washed with PSS 0Ca before recordings. Baseline fluorescence (excitation 360 nm, emission 510 nm) was acquired using a FlexStation 3 microplate reader (Molecular Devices). After, $MnCl_2$ was added to a final concentration of 5 mM. Constitutive Ca^{2+} entry was quantified as the absolute slope of fluorescence decay during the 100s following Mn^{2+} addition.

2.6. Mitochondrial Ca^{2+} Imaging

Mitochondrial Ca^{2+} transients were measured using Rhod-2-AM/Mitotracker green (Thermo Fisher Scientific) fluorescence dye (excitation/emission: 543 nm/580–650 nm). HEK-293 cells were seeded on glass coverslips and used at 60–70% confluency for imaging. Prior to acquisition, cells were loaded for 30 min at room temperature with 1 µM Rhod-2-AM. Cells were then washed three times with Ca^{2+}-containing PSS (PSS 2Ca) and maintained in a similar buffer during recording. Ca^{2+} transients were induced by addition of ionomycin (1 µM) after 50s of baseline acquisition. Imaging was performed using a Leica TCS SP8 confocal microscope, and fluorescence intensity was analyzed using LAS X software

(Leica Microsystems). COV504, COV504 CP and COV504 TX cells were loaded in black 96 plates (CellStar™, Greiner Bio-One) at a 30 000 cells/well density for 30 minutes with Rhod-2 AM (2 µM) in Opti-MEM medium at 37°C, 5% CO_2. After loading, the Opti-MEM medium was replaced with PSS 2Ca. Ca^{2+} transients were induced by addition of ionomycin (1 µM). The maximal fluorescence obtained after Ionomycin injection (Rmax) in each well was compared to baseline (R_0) to calculate the amplitude (Rmax – R_0), reflecting mitochondrial Ca^{2+} uptake.

2.7. mPTP sensitivity

Mitochondrial permeability transition pore (mPTP) opening was assessed using the $CoCl_2$–calcein quenching assay (Bonora et al., 2016). Cells were loaded with calcein-AM (Thermo Fisher Scientific, 2 µM) for 30 min at 37°C in a humidified atmosphere with 5% CO_2. Subsequent addition of $CoCl_2$ (2 mM) in PSS 0.5Ca selectively quenched cytosolic fluorescence, allowing mitochondrial calcein signal to be monitored. After reaching a stable baseline, ionomycin (10 µM) was added to induce mitochondrial permeabilization and promote mPTP opening. The rate of fluorescence decay following ionomycin addition was quantified, and results are expressed as the absolute value of the slope. Cyclosporin A (CsA) (4 µM), an inhibitor of mPTP opening, was used as a positive control.

2.8. RNA isolation and Real-Time Quantitative RT-PCR

Total RNA extraction (NucleoSpin® RNA Plus kit, Macherey-Nagel, Hoerdt, France), reverse transcription (PrimeScript RT kit, Takara, Saint Germain en Laye, France) and amplification (TB green Premix ExTaq kit, Takara) were performed as described previously (Romito et al., 2024). The experiments were performed on CFX Maestro from Bio-Rad (Marnes la Coquette, France). Quantitative real-time PCR (qRT-PCR) was performed in duplicate using 25 ng of cDNA and gene-specific primers (see below). Relative expression levels were calculated using the comparative Ct method and fold changes were calculated using the 2^−ΔΔCt method. Expression levels were normalized using four housekeeping genes (HPRT1, ALAS1, TBP, and RNF181). The following primer sequences were used:

Gene Forward Reverse

Orai1 5’AGGTGATGAGCCTCAACGAG 3’ 5’ CTGATCATGAGCGCAAACAG 3’

Orai2 5’ CTCGCTGATGGAGTTCAGGT 3’ 5’ TGGATTACCGGGACTGGGT 3’

Orai3 5’ACTCGTGGTCACTCTCCAGC 3’ 5’ CCACGTACCGGGAGTTCG 3’

STIM1 5' GCCCTCAACATAGACCCCAG 3' 5' TCCATGTCATCCACGTCGTCA 3'

STIM2 5' TTGGACCCTTGAAGACACTCT 3' 5' CCAGTTATGAGGTGGGCGTG 3'

SK1 5’ CACCAAGGAGTCTCTGTACTC 3’ 5’ CAGTCATCAGCCCCGTTGT 3’

SK2 5’ GACTTGGCAAAGACCCAGAA 3’ 5’ CCGCTCAGCATTGTAAGTGA 3’

SK3 5’ TGGACACTCAGCTCACCAAG 3’ 5’ GTTCCATCTTGACGCTCCTC 3’

TRPC1 5’ TGGGATGATTTGGTCAGACA 3’ 5’ TCTGCCACCAGTGTACCATG 3’

TRPC3 5’ CTTTCCTTCAGGCAACGAAC 3’ 5’ GTACGCAATCCGAGAGAAGC 3’

TRPC4 5’ AACAATAGGGAGGCGAGCTG 3’ 5’ TCCCAGGACTTCAAAGCGGA 3’

TRPC5 5’ CAACTGTCGTGGAATGGATG 3’ 5’CCCTTGGACGAGAACCATTA 3’

TRPC6 5’ GGATTACATGGGCCAGAATG 3’ 5’ GCTGGTTGCTAACCTCTTGC 3’

MCU 5' CGCCAGGAATATGTTTATCCA 3' 5' CTTGTAATGGGTCTCTCAGTCTGTT 3'

MICU1 5'GAGGCAGCTCAAGAAGCACT 3' 5' CAAACACCACATCACACACG 3'

MICU2 5' GGCAGTTTTACAGTCTCCGC 3' 5' AAGAGGAAGTCTCGTGGTGTC 3'

NCLX (SLC8B1) 5' GCCAGCATTTGTGTCCATTT 3' 5'AATTCGTCTCGGCCACTTAC 3'

HPRT1 5’ TGACCTTGATTTATTTTGCATACC 3’ 5’ CGAGCAAGACGTTCAGTCCT 3’

TBP 5’ TGTATCCACAGTGAATCTTGGTTG 3’ 5’ GGTTCGTGGCTCTCTTATCCTC 3’

ALAS1 5’ AGATCTGACCCCTCAGTCCC 3’ 5’ TCCACGAAGGTGATTGCTCC 3’

h-RNF-181 5’ GGGCCAGGAGCATAAGTACC 3’ 5’ ATCAGGAGGGCTCTCATCCA 3’

2.9. Bioinformatics and survival analyses

Gene expression levels of *ORAI1* across ovarian cancer stages were analyzed using GEPIA (Gene Expression Profiling Interactive Analysis) based on TCGA ovarian serous cystadenocarcinoma (OV) datasets. Associations between gene expression and patient outcomes were evaluated using the Kaplan–Meier Plotter database (kmplot.com), incorporating serous ovarian cancer cohorts treated with platinum-based chemotherapy. Progression-free survival (PFS) and overall survival (OS) were assessed using mRNA expression data integrated from GEO, EGA, and TCGA datasets. Patients were stratified into high- and low-expression groups using the automatically selected best cutoff. Survival differences were analyzed using Kaplan–Meier estimates and compared using the log-rank test, with hazard ratios (HR) and 95% confidence intervals (CI) reported.

2.10. Pharmacology

Carboplatin (water) was obtained graciously from Hopital Bretonneau, Tours, France with the help of Lobna Ouldamer. Taxol® (DMSO), Morusin (DMSO), Ionomycin (DMSO) and Cyclosporin A (DMSO) were purchased from Sigma-Aldrich (Saint Quentin Fallavier, France).

2.11. Statistics

We used GraphPad Prism 11 (https://www.graphpad.com/) for statistical analyses. Data are presented as mean ± SEM. All comparisons were performed using either Mann-Whitney (two tailed) or one-way Anova (Tukey post-hoc). Statistical significance was established for $P < 0.05$*, $P < 0.01$**, $P < 0.001$***, $P < 0.0001$****.

3. Results

3.1. Ca^{2+} signaling is selectively remodeled in carboplatin-resistant, but not in Taxol®-resistant, COV504 cells

Resistant sublines (COV504 CP and COV504 TX) were validated using the MTT assay, confirming a significant increase in EC_{50} for carboplatin and Taxol®, relative to parental COV504 cells (Fig. 1A–D). We next examined SOCE using the classical thapsigargin protocol. Thapsigargin (4 μM)-induced ER Ca^{2+} store depletion was unchanged between COV504 and COV504 TX, but was significantly reduced in COV504 CP (Fig. 1E-J). Consistently, Ca^{2+} re-addition-following ER store depletion elicited a robust SOCE response in COV504 TX, whereas SOCE was significantly blunted in COV504 CP cells (Fig. 1E-J). These findings were corroborated using lysophosphatidic acid (LPA, 10 μM), a physiological relevant SOCE trigger to ovarian cancer aggressiveness (Pua et al., 2009; Xu, 1998) (Fig. 1K–P). We next investigated CCE, using the Mn^{2+} quench method. CCE was significantly reduced in COV504 CP cells, whereas it remained unchanged in COV504 TX cells compared with parental COV504 cells (Fig. 1Q-T). Finally, we assessed mitochondrial Ca^{2+} uptake following ionomycin stimulation (1 μM) using the mitochondrial Ca^{2+} indicator Rhod-2 AM. Ionomycin-induced mitochondrial Ca^{2+} uptake was significantly reduced in COV504 CP cells relative to parental cells, whereas no significant difference was observed in COV504 TX cells (Fig. 1U-X).

Collectively, these results indicate that acquired carboplatin resistance is associated with a broad reduction in Ca^{2+} mobilization and entry, encompassing ER Ca^{2+} release, SOCE, CCE, and mitochondrial Ca^{2+} uptake, whereas these Ca^{2+} signaling pathways remain largely preserved in Taxol®-resistant cells.

Alt text

Analysis of plasma membrane and mitochondrial Ca^{2+} pathway in carboplatin or Taxol®-resistant high grade serous ovarian cancer cells.

3.2. Carboplatin sensitizes the mPTP to limit mitochondrial Ca^{2+} overload

We assessed the mPTP opening using the calcein-$CoCl_2$ quench assay, validated with the mPTP inhibitor CsA (Fig. 2). Ionomycin-induced calcein quenching (10 μM), reflecting mPTP opening, was significantly faster in COV504 CP than in parental COV504 or COV504 TX cells, indicating increased mPTP sensitivity specifically in carboplatin-resistant cells (Fig. 2A-D). Because COV504 CP cells are continuously

maintained in 10 μM carboplatin to preserve the resistant phenotype, we asked whether this increased mPTP sensitivity reflected a stable adaptation or an ongoing effect of carboplatin exposure. To distinguish between these possibilities, non-malignant HEK-293 cells, which had not been previously exposed to carboplatin and did not exhibit Ca^{2+} signaling remodeling, were treated with carboplatin (50 μM, 24 h). This short-term exposure was sufficient to reproduce the mPTP hypersensitivity observed in COV504 CP cells (Fig. 2E and 2F), indicating that carboplatin rapidly sensitizes the mPTP.

We then investigated whether mPTP sensitization might contribute to limiting mitochondrial Ca^{2+} accumulation rather than promoting cell death. Morusin, a flavonoid reported to promote mitochondrial Ca^{2+} overload in ovarian cancer (Xue et al., 2018), prevented carboplatin-induced mPTP sensitization in HEK-293 (Fig. 2E and 2F). This was accompanied by increased basal mitochondrial Ca^{2+} concentration (Fig. 2G-I), and significant enhancement of carboplatin-induced cytotoxicity (Fig. 2J and 2K). (Fig. 2J and 2K). Thus, pharmacological attenuation of mPTP sensitization increased mitochondrial Ca^{2+} accumulation while potentiating carboplatin cytotoxicity, consistent with the possibility that early mPTP sensitization contributes to the maintenance of mitochondrial Ca^{2+} homeostasis and limits Ca^{2+} overload following carboplatin exposure. Morusin enhanced carboplatin cytotoxicity in COV504 CP as well (Fig. 2L and 2M), further supporting a functional link between mitochondrial Ca^{2+} handling, mPTP regulation, and platinum sensitivity.

These findings identify the mPTP–mitochondrial Ca^{2+} axis as a potential vulnerability that could be exploited to enhance carboplatin efficacy in platinum-resistant ovarian cancer cells.

Alt text

Modulation of mPTP, mitochondrial Ca^{2+} and cell survival in carboplatin or Taxol®-resistant cells, as well as HEK-293.

3.3 **Carboplatin resistance cells exhibit a selective downregulation of plasma membrane and mitochondrial Ca^{2+} channels and low ORAI1 expression predicts poor outcome.**

To determine whether the functional Ca^{2+} remodeling observed in COV504 CP cells was associated with transcriptional changes in the Ca^{2+} signaling machinery, we quantified the expression of key Ca^{2+} channels and transporters by qRT-PCR. COV504 CP cells exhibited a significant downregulation of several components of the SOCE and CCE machinery, including *Orai1* and *STIM1* (Fig. 3A and 3E). In addition, the expression of *KCNN2* and *KCNN3*, encoding the small-conductance Ca^{2+}-activated K^+ channels SK2 and SK3, which have been implicated in the regulation of SOCE and CCE (Guéguinou et al., 2016; Romito et al., 2024), was significantly reduced (Fig. 3A and 3E). MCU expression, encoding the pore-forming subunit of the mitochondrial Ca^{2+} uniporter (Liu et al., 2020), was also significantly decreased (Fig. 3C,G). These transcriptional changes were consistent with the reduced SOCE, CCE, and mitochondrial Ca^{2+} uptake observed in COV504 CP cells (Fig. 1). In contrast, COV504 TX cells, which displayed preserved Ca^{2+} entry and mitochondrial Ca^{2+} uptake (Fig. 1), showed no significant changes in the expression of *Orai1*, *Orai2*, *Orai3*, *STIM1*, *STIM2*, *TRPC3*, *TRPC5*, *MCU*, *MICU1*, *MICU2*, or *SLC8B1*.

However, *TRPC4* and *TRPC6* expression was significantly increased (Fig. 3B,D,F,H), as were *KCNN1*, *KCNN2*, and *KCNN3* (Romito et al., 2024). Despite these transcriptional changes, the functional parameters of SOCE, CCE, and mitochondrial Ca^{2+} uptake remained unchanged in COV504 TX cells (Fig. 1), indicating that these alterations do not result in detectable changes in the Ca^{2+} entry pathways examined.

We next investigated the clinical relevance of altered *ORAI1* expression using publicly available transcriptomic and clinical datasets. Analysis of GEPIA (GEPIA (Gene Expression Profiling Interactive Analysis) revealed significantly lower *ORAI1* mRNA expression in advanced-stage ovarian tumors compared with earlier-stage disease (Fig. 3I, and 3J). Consistently, Kaplan–Meier Plotter analysis showed that lower tumoral *ORAI1* expression was associated with shorter progression-free survival (PFS) and overall survival (OS), especially in early stages (1 + 2), among ovarian cancer patients receiving platinum-based treatment (Fig. 3K–N).

Altogether, these data support the idea that carboplatin resistance is associated with coordinated transcriptional downregulation of components involved in plasma membrane Ca^{2+} entry and mitochondrial Ca^{2+} uptake, consistent with the functional Ca^{2+} remodeling observed in COV504 CP cells. Notably, reduced *ORAI1* expression was associated with advanced disease and poorer clinical outcome following platinum-based treatment, supporting the clinical relevance of this Ca^{2+} signaling remodeling.

Alt text

mRNA expression of Ca^{2+} channels in carboplatin or Taxol®-resistant high grade serous ovarian cancer, followed by *Orai1* clinical relevance in ovarian cancer progression.

4. Discussion

Our findings support a two-step model of Ca^{2+} signaling adaptation to carboplatin in ovarian cancer cells. First, carboplatin exposure rapidly sensitizes the mPTP, an effect that can be observed following short-term treatment in non-malignant cells. Second, cells that survive chronic carboplatin exposure and acquire resistance retain this increased mPTP sensitivity while undergoing coordinated downregulation of multiple components of the Ca^{2+} signaling machinery. Notably, this broader Ca^{2+} remodeling was not observed in Taxol®-resistant cells, pointing to a platinum-specific adaptive response rather than a general consequence of chemotherapy resistance.

The direct sensitization of the mPTP by carboplatin observed in non-cancerous HEK-293 cells is consistent with previous reports showing that platinum agents can increase the sensitivity of mitochondria to Ca^{2+}-induced permeability transition (Chen et al., 2013; Custódio et al., 2009; Kim et al., 2025). Cisplatin, in particular, has been shown to sensitize the mPTP in isolated liver mitochondria independently of any tumor-specific context (Custódio et al., 2009). Conversely, alterations in mPTP regulation have been implicated in multidrug resistance in hepatocellular carcinoma cells (Ling et al., 2010), while cisplatin-induced cell death in pancreatic cancer cells has been reported to depend on

cyclophilin D, a core regulatory component of the mPTP (Chen et al., 2013). Together, these observations support the notion that platinum-induced mPTP sensitization may represent a direct pharmacological effect shared across cellular contexts, rather than a phenotype uniquely acquired by the COV504 model. Our findings therefore extend previous work by linking this early mitochondrial response to the subsequent remodeling of Ca^{2+} signaling associated with acquired carboplatin resistance.

At first sight, increased mPTP sensitivity might be expected to promote cell death, as a lower threshold for pore opening generally increases mitochondrial susceptibility to Ca^{2+}-dependent permeability transition (Kinnally et al., 2011; Robichaux et al., 2023; Zhao et al., 2022). However, the mPTP is also known to open transiently, in a low-conductance "flickering" mode (Agarwal et al., 2017) that allows Ca^{2+} efflux from the matrix without triggering sustained, lethal permeability transition, and this mode has been proposed to act as a physiological safety valve limiting mitochondrial Ca^{2+} overload in several tissues (Bernardi et al., 2023; Hurst et al., 2017; J. Liu et al., 2025). Our pharmacological data are consistent with this alternative interpretation. Morusin reduced carboplatin-induced mPTP sensitization and concomitantly increased basal mitochondrial Ca^{2+} levels and carboplatin cytotoxicity. Thus, under our experimental conditions, attenuation of mPTP sensitization was associated with greater mitochondrial Ca^{2+} accumulation and enhanced cell death, suggesting that increased mPTP sensitivity may, at least in part, facilitate Ca^{2+} release and thereby limit mitochondrial Ca^{2+} overload. We therefore speculate that carboplatin-induced mPTP sensitization could reflect an increased propensity for transient, flickering pore openings that function as an early adaptive response to mitochondrial Ca^{2+} stress. However, because pore conductance and opening dynamics were not directly measured in the present study, this interpretation remains hypothetical and will require direct assessment of mPTP activity, ideally using approaches capable of resolving pore conductance and opening kinetics.

Within this framework, the downregulation of *Orai1*, *STIM1*, *KCNN2*, *KCNN3*, and *MCU* observed in COV504 CP cells may represent a second, complementary layer of adaptation. By reducing Ca^{2+} entry and mitochondrial Ca^{2+} uptake, carboplatin-resistant cells may limit the amount of Ca^{2+} delivered to mitochondria, thereby reducing the burden imposed on an already sensitized mPTP. In this context, the concomitant decrease in *KCNN2*/*KCNN3* alongside *Orai1* and *STIM1* is consistent with the functional coupling between SKCa channels and Orai-dependent Ca^{2+} entry described in other cancer models contexts (Chantôme et al., 2013; Guéguinou et al., 2016, 2014). This is further supported by our previous work in the COV504 cell line, showing that SK2 directly regulates SOCE and that low *KCNN2* expression is associated with shorter progression-free survival in patients with serous ovarian cancer (Romito et al., 2024). Similarly, reduced *KCNN3* expression has been associated with poorer clinical outcome in ovarian cancer patients (Liu et al., 2018). The potential clinical relevance of this Ca^{2+} remodeling is further supported by our analysis of patient datasets. *Orai1* mRNA expression progressively decreased with increasing ovarian cancer stage, and low tumoral expression of *Orai1* was associated with shorter progression-free and overall survival in patients with serous ovarian cancer receiving platinum-based chemotherapy. These clinical observations parallel the reduced *Orai1* expression observed in COV504 CP cells and suggest that reduction of the SOCE machinery may be associated with advanced and platinum-resistant ovarian cancer. Although these associations do not establish a causal relationship, their

concordance with our experimental findings supports the biological relevance of this Ca^{2+} signaling phenotype beyond the COV504 model.

The direction of this remodeling nevertheless differs from previous reports describing increased Orai1 expression in cisplatin-resistant ovarian cancer cells, in which enhanced SOCE promoted an anti-apoptotic pathway (Huang et al., 2020; Schmidt et al., 2014). More broadly, Orai1 have been implicated in chemoresistance across several cancer types (Romito et al., 2022). This apparent discrepancy may reflect differences in the cellular and molecular mechanisms underlying resistance rather than a fundamental contradiction. Cisplatin and carboplatin differ in their chemical reactivity, intracellular processing, and pharmacological properties, which may influence the adaptive pathways selected during chronic exposure (Dasari and Bernard Tchounwou, 2014). Moreover, platinum resistance is a heterogeneous phenotype that can arise through multiple, non-mutually exclusive mechanisms and is strongly influenced by cellular and genetic context (Dasari and Bernard Tchounwou, 2014). Our findings therefore suggest that Ca^{2+} signaling may undergo divergent forms of remodeling during the acquisition of platinum resistance. In some contexts, increased SOCE may sustain pro-survival and anti-apoptotic signaling, whereas in others, suppression of Ca^{2+} entry may limit mitochondrial Ca^{2+} accumulation and thereby reduce the consequences of an intrinsically sensitized mPTP. The balance between these opposing adaptations may depend on the nature of the platinum compound, the cellular background, and the mitochondrial death pathways exerting the dominant selective pressure during treatment.

Our findings echo those reported by Xue et al., who showed that morusin, a flavonoid isolated from the root bark of *Morus australis*, induces mitochondrial Ca^{2+} uptake in epithelial ovarian cancer cells, accompanied by ER stress marker accumulation, ROS production, and loss of mitochondrial membrane potential, ultimately leading to mitochondrial Ca^{2+} overload and cell death (Xue et al., 2018). In the present study, we showed that low concentration of morusin similarly increased basal mitochondrial Ca^{2+} when combined with carboplatin. Our data further suggest that this effect is due to a modification in mPTP sensitization threshold, thereby favoring mitochondrial Ca^{2+} accumulation and enhancing carboplatin-induced cytotoxicity. This mode of action may represent a particularly relevant therapeutic strategy in a context of acquired platinium resistance in which adaptive remodeling of Ca^{2+} signaling may limit mitochondrial Ca^{2+} accumulation and thereby reduce the effectiveness of chemotherapy. Pharmacological modulation of the mPTP/Ca^{2+} axis may therefore represent a potential strategy to enhance carboplatin-induced cell death in resistant ovarian cancer cells.

Several limitations should be acknowledged. The proposed link between mPTP sensitization and a protective, flickering-type mechanism, remains indirect and is based primarily on pharmacological manipulation rather than direct measurements of pore conductance or opening kinetics. The specific contribution of Ca^{2+} channels to the observed functional phenotypes remains to be determined using targeted loss- and gain-of-function approaches. Finally, the relationship between Ca^{2+} signaling remodeling and mPTP regulation remains largely correlative. Establishing causality will require direct manipulation of mitochondrial Ca^{2+} handling and/or mPTP components, together with real-time assessment of mitochondrial Ca^{2+} dynamics and pore activity.

5. Conclusion

These findings suggest that carboplatin resistance in ovarian cancer cells involves a deep Ca^{2+} remodeling, with acute sensitization of the mPTP that may act as an early protective mechanism against Ca^{2+} overload, reinforced in resistant cells by a coordinated downregulation of the Ca^{2+} entry and mitochondrial Ca^{2+} machinery. Morusin, by disabling this protective mPTP response and promoting mitochondrial Ca^{2+} accumulation, enhances carboplatin cytotoxicity, highlighting mitochondrial Ca^{2+} handling as a candidate vulnerability of carboplatin-resistant ovarian cancer cells.

Declarations

1. ***Data availability***

The dataset supporting the conclusions of this article is included within the article and its additional file.

2. ***Conflict of interest***

Mohamed Trebak is a paid consultant of Seeker Biologics Inc.

3. ***Authors contribution***

OR wrote the manuscript that was critically reviewed by MP-C, CG and MT. OR, OC, and AL performed the experiments. MP-C, CG and MT supervised the project.

4. ***Funding and acknowledgements***

This study was supported by grants from the University of Tours, the Région Centre-Val de Loire, INSERM, Canceropôle Grand Ouest, the Ligue Nationale Contre le Cancer, the Association CANCEN, the association of oncology Tours' Hospital ACORT. We thank Murielle Genty, Catherine Leroy and Sophie Hamard for secretarial support. The authors thank Dr Nadine Hempel's laboratory which kindly provided COV504 cell line.

References

1. Agarwal A, Wu P-H, Hughes EG, Fukaya M, Tischfield MA, Langseth AJ, Wirtz D, Bergles DE. Transient Opening of the Mitochondrial Permeability Transition Pore Induces Microdomain Calcium Transients in Astrocyte Processes. Neuron. 2017;93:587–e6057. https://doi.org/10.1016/j.neuron.2016.12.034.
2. Al-Taweel N, Varghese E, Florea A-M, Büsselberg D. Cisplatin (CDDP) triggers cell death of MCF-7 cells following disruption of intracellular calcium ($[Ca^{2+}]_i$) homeostasis. J Toxicol Sci. 2014;39:765–74. https://doi.org/10.2131/jts.39.765.

3. Arbel N, Shoshan-Barmatz V. Voltage-dependent Anion Channel 1-based Peptides Interact with Bcl-2 to Prevent Antiapoptotic Activity. J Biol Chem. 2010;285:6053–62. https://doi.org/10.1074/jbc.M109.082990.
4. Bernardi P, Gerle C, Halestrap AP, Jonas EA, Karch J, Mnatsakanyan N, Pavlov E, Sheu S-S, Soukas AA. Identity, structure, and function of the mitochondrial permeability transition pore: controversies, consensus, recent advances, and future directions. Cell Death Differ. 2023;30:1869–85. https://doi.org/10.1038/s41418-023-01187-0.
5. Bernardi P, Von Stockum S. The permeability transition pore as a Ca2 + release channel: New answers to an old question. Cell Calcium. 2012;52:22–7. https://doi.org/10.1016/j.ceca.2012.03.004.
6. Bonora M, Morganti C, Morciano G, Giorgi C, Wieckowski MR, Pinton P. Comprehensive analysis of mitochondrial permeability transition pore activity in living cells using fluorescence-imaging-based techniques. Nat Protoc. 2016;11:1067–80. https://doi.org/10.1038/nprot.2016.064.
7. Bravo-Sagua R, Parra V, López-Crisosto C, Díaz P, Quest AFG, Lavandero S. Calcium Transport and Signaling in Mitochondria. In: Terjung R, editor. Comprehensive Physiology. Wiley; 2017. pp. 623–34. https://doi.org/10.1002/cphy.c160013.
8. Chantôme A, Potier-Cartereau M, Clarysse L, Fromont G, Marionneau-Lambot S, Guéguinou M, Pagès J-C, Collin C, Oullier T, Girault A, Arbion F, Haelters J-P, Jaffrès P-A, Pinault M, Besson P, Joulin V, Bougnoux P, Vandier C. Pivotal Role of the Lipid Raft SK3–Orai1 Complex in Human Cancer Cell Migration and Bone Metastases. Cancer Res. 2013;73:4852–61. https://doi.org/10.1158/0008-5472.CAN-12-4572.
9. Chatelut É. Pharmacologie des dérivés du platine: différences entre les trois composés et les facteurs de variabilité entre patients. Bull Cancer. 2011;98:1253–61. https://doi.org/10.1684/bdc.2011.1464.
10. Chen B, Xu M, Zhang H, Wang J, Zheng P, Gong L, Wu G, Dai T. Cisplatin-induced non-apoptotic death of pancreatic cancer cells requires mitochondrial cyclophilin-D-p53 signaling. Biochem Biophys Res Commun. 2013;437:526–31. https://doi.org/10.1016/j.bbrc.2013.06.103.
11. Custódio JBA, Cardoso CMP, Santos MS, Almeida LM, Vicente JAF, Fernandes MAS. Cisplatin impairs rat liver mitochondrial functions by inducing changes on membrane ion permeability: Prevention by thiol group protecting agents. Toxicology. 2009;259:18–24. https://doi.org/10.1016/j.tox.2009.01.022.
12. Dalton WS, Crowley JJ, Salmon SS, Grogan TM, Laufman LR, Weiss GR, Bonnet JD. A phase III randomized study of oral verapamil as a chemosensitizer to reverse drug resistance in patients with refractory myeloma. A southwest oncology group study. Cancer. 1995;75(1995020175):815–20. https://doi.org/10.1002/1097-0142. :3%3C815::AID-CNCR2820750311%3E3.0.CO;2-R.
13. Dasari S, Bernard Tchounwou P. Cisplatin in cancer therapy: Molecular mechanisms of action. Eur J Pharmacol. 2014;740:364–78. https://doi.org/10.1016/j.ejphar.2014.07.025.

14. Eubler K, Jeevanandan SP, Caban KM, Stöckl JB, Braun MB, Herrmann C, Schneider M, Kreitmair N, Scholz L, Mayr D, Renkawitz J, Welter H, Müller-Taubenberger A, Fröhlich T, Mayerhofer A. TRPV2 regulates cell fate in the human granulosa-like tumor cell line KGN: implications for granulosa cell tumors and cannabidiol. Cell Commun Signal. 2026;24:139. https://doi.org/10.1186/s12964-026-02729-y.
15. Flourakis M, Lehen'kyi V, Beck B, Raphaël M, Vandenberghe M, Abeele FV, Roudbaraki M, Lepage G, Mauroy B, Romanin C, Shuba Y, Skryma R, Prevarskaya N. Orai1 contributes to the establishment of an apoptosis-resistant phenotype in prostate cancer cells. Cell Death Dis. 2010;1:e75–75. https://doi.org/10.1038/cddis.2010.52.
16. Guéguinou M, Chantôme A, Fromont G, Bougnoux P, Vandier C, Potier-Cartereau M. KCa and Ca2 + channels: The complex thought. Biochimica et Biophysica Acta (BBA) -. Mol Cell Res. 2014;1843:2322–33. https://doi.org/10.1016/j.bbamcr.2014.02.019.
17. Guéguinou M, Harnois T, Crottes D, Uguen A, Deliot N, Gambade A, Chantôme A, Haelters JP, Jaffrès PA, Jourdan ML, Weber G, Soriani O, Bougnoux P, Mignen O, Bourmeyster N, Constantin B, Lecomte T, Vandier C, Potier-Cartereau M. SK3/TRPC1/Orai1 complex regulates SOCE-dependent colon cancer cell migration: a novel opportunity to modulate anti-EGFR mAb action by the alkyl-lipid Ohmline. Oncotarget. 2016;7:36168–84. https://doi.org/10.18632/oncotarget.8786.
18. Hasna J, Hague F, Rodat-Despoix L, Geerts D, Leroy C, Tulasne D, Ouadid-Ahidouch H, Kischel P. Orai3 calcium channel and resistance to chemotherapy in breast cancer cells: the p53 connection. Cell Death Differ. 2018;25:693–707. https://doi.org/10.1038/s41418-017-0007-1.
19. Huang H-K, Lin Y-H, Chang H-A, Lai Y-S, Chen Y-C, Huang S-C, Chou C-Y, Chiu W-T. Chemoresistant ovarian cancer enhances its migration abilities by increasing store-operated Ca2 + entry-mediated turnover of focal adhesions. J Biomed Sci. 2020;27:36. https://doi.org/10.1186/s12929-020-00630-5.
20. Hurst S, Hoek J, Sheu S-S. Mitochondrial Ca2 + and regulation of the permeability transition pore. J Bioenerg Biomembr. 2017;49:27–47. https://doi.org/10.1007/s10863-016-9672-x.
21. Kim Y-R, Jun S, Jung S, Lee B, Lee S-H, Lee J, Hwang J-S, Thoudam T, Lee H, Sinam IS, Jeon J-H, Lee K-Y, Min S-J, Kim U-K. Inhibition of the mitochondrial permeability transition pore as a promising target for protecting auditory function in cisplatin-induced hearing loss. Biomed Pharmacother. 2025;182:117767. https://doi.org/10.1016/j.biopha.2024.117767.
22. Kinnally KW, Peixoto PM, Ryu S-Y, Dejean LM. Is mPTP the gatekeeper for necrosis, apoptosis, or both? Biochimica et Biophysica Acta (BBA) -. Mol Cell Res. 2011;1813:616–22. https://doi.org/10.1016/j.bbamcr.2010.09.013.
23. Kondratska K, Kondratskyi A, Yassine M, Lemonnier L, Lepage G, Morabito A, Skryma R, Prevarskaya N. Orai1 and STIM1 mediate SOCE and contribute to apoptotic resistance of pancreatic adenocarcinoma. Biochimica et Biophysica Acta (BBA) -. Mol Cell Res. 2014;1843:2263–9. https://doi.org/10.1016/j.bbamcr.2014.02.012.

24. Ling X, Zhou Y, Li S-W, Yan B, Wen L. Modulation of Mitochondrial Permeability Transition Pore Affects Multidrug Resistance in Human Hepatocellular Carcinoma Cells. Int J Biol Sci. 2010;773–83. https://doi.org/10.7150/ijbs.6.773.
25. Liu J, Wu C, Lin Z, Ma M, Ma W, Yu X, Wang K, Zeng B. Cyclophilin D (PPIF) and MPTP in hepatic ischemia-reperfusion injury: insights into mechanisms. Front Immunol. 2025;16:1575242. https://doi.org/10.3389/fimmu.2025.1575242.
26. Liu O, Hu Y, Wang S, Nie X, Wang Y, Fan X, Zeng K, Li X, Liu B, Lin B. MRPL13 enhances mitochondrial function and promotes tumor progression in ovarian cancer by inhibiting mPTP opening via SLC25A6. Cell Death Dis. 2025;16:634. https://doi.org/10.1038/s41419-025-07953-x.
27. Liu X, Wei L, Zhao B, Cai X, Dong C, Yin F. Low expression of KCNN3 may affect drug resistance in ovarian cancer. Mol Med Rep. 2018. https://doi.org/10.3892/mmr.2018.9107.
28. Liu Y, Jin M, Wang Y, Zhu J, Tan R, Zhao J, Ji X, Jin C, Jia Y, Ren T, Xing J. MCU-induced mitochondrial calcium uptake promotes mitochondrial biogenesis and colorectal cancer growth. Sig Transduct Target Ther. 2020;5:59. https://doi.org/10.1038/s41392-020-0155-5.
29. Marchi S, Patergnani S, Missiroli S, Morciano G, Rimessi A, Wieckowski MR, Giorgi C, Pinton P. Mitochondrial and endoplasmic reticulum calcium homeostasis and cell death. Cell Calcium. 2018;69:62–72. https://doi.org/10.1016/j.ceca.2017.05.003.
30. Marchi S, Pinton P. Mitochondrial calcium uniporter, MiRNA and cancer: Live and let die. Commun Integr Biol. 2013;6:e23818. https://doi.org/10.4161/cib.23818.
31. Mohr CJ, Steudel FA, Gross D, Ruth P, Lo W-Y, Hoppe R, Schroth W, Brauch H, Huber SM, Lukowski R. 2019. Cancer-Associated Intermediate Conductance Ca2+-Activated K+ Channel KCa3.1. Cancers 11, 109. https://doi.org/10.3390/cancers11010109
32. Ozols RF, Bundy BN, Greer BE, Fowler JM, Clarke-Pearson D, Burger RA, Mannel RS, DeGeest K, Hartenbach EM, Baergen R. 2003. Phase III Trial of Carboplatin and Paclitaxel Compared With Cisplatin and Paclitaxel in Patients With Optimally Resected Stage III Ovarian Cancer: A Gynecologic Oncology Group Study. JCO 21, 3194–3200. https://doi.org/10.1200/JCO.2003.02.153
33. Protasoni M, López-Polo V, Stephan-Otto Attolini C, Brandariz J, Herranz N, Mateo J, Ruiz S, Fernandez-Capetillo O, Kovatcheva M, Serrano M. Cyclophilin D plays a critical role in the survival of senescent cells. EMBO J. 2024;43:11. https://doi.org/10.1038/s44318-024-00259-2.
34. Pua TL, Wang F, Fishman DA. Roles of LPA in ovarian cancer development and progression. Future Oncol. 2009;5:1659–73. https://doi.org/10.2217/fon.09.120.
35. Robichaux DJ, Harata M, Murphy E, Karch J. Mitochondrial permeability transition pore-dependent necrosis. J Mol Cell Cardiol. 2023;174:47–55. https://doi.org/10.1016/j.yjmcc.2022.11.003.
36. Romito O, Guéguinou M, Raoul W, Champion O, Robert A, Trebak M, Goupille C, Potier-Cartereau M. Calcium signaling: A therapeutic target to overcome resistance to therapies in cancer. Cell Calcium. 2022;108:102673. https://doi.org/10.1016/j.ceca.2022.102673.
37. Romito O, Lemettre A, Chantôme A, Champion O, Couty N, Ouldamer L, Hempel N, Trebak M, Goupille C, Potier-Cartereau M. Plasma membrane SK2 channel activity regulates migration and

chemosensitivity of high-grade serous ovarian cancer cells. Mol Oncol. 2024;18:1853–65. https://doi.org/10.1002/1878-0261.13631.

38. Schmidt S, Liu, Guoxing, Liu, Guilai, Yang W, Honisch S, Pantelakos S, Stournaras C, Hönig A, Lang F. Enhanced Orai1 and STIM1 expression as well as store operated Ca2 + entry in therapy resistant ovary carcinoma cells. Oncotarget. 2014;5:4799–810. https://doi.org/10.18632/oncotarget.2035.
39. Siddik ZH. Cisplatin: mode of cytotoxic action and molecular basis of resistance. Oncogene. 2003;22:7265–79. https://doi.org/10.1038/sj.onc.1206933.
40. Sung H, Ferlay J, Siegel RL, Laversanne M, Soerjomataram I, Jemal A, Bray F. Global Cancer Statistics 2020: GLOBOCAN Estimates of Incidence and Mortality Worldwide for 36 Cancers in 185 Countries. CA Cancer J Clin. 2021;71:209–49. https://doi.org/10.3322/caac.21660.
41. Tajeddine N, Galluzzi L, Kepp O, Hangen E, Morselli E, Senovilla L, Araujo N, Pinna G, Larochette N, Zamzami N, Modjtahedi N, Harel-Bellan A, Kroemer G. Hierarchical involvement of Bak, VDAC1 and Bax in cisplatin-induced cell death. Oncogene. 2008;27:4221–32. https://doi.org/10.1038/onc.2008.63.
42. Tang B-D, Xia X, Lv X-F, Yu B-X, Yuan J-N, Mai X-Y, Shang J-Y, Zhou J-G, Liang S-J, Pang R-P. Inhibition of Orai1-mediated Ca $^{2+}$ entry enhances chemosensitivity of HepG2 hepatocarcinoma cells to 5-fluorouracil. J Cell Mol Med. 2017;21:904–15. https://doi.org/10.1111/jcmm.13029.
43. Xu Y. Lysophosphatidic Acid as a Potential Biomarker for Ovarian and Other Gynecologic Cancers. JAMA. 1998;280:719. https://doi.org/10.1001/jama.280.8.719.
44. Xu Y, Wang C, Su J, Xie Q, Ma L, Zeng L, Yu Y, Liu S, Li S, Li Z, Sun L. Tolerance to endoplasmic reticulum stress mediates cisplatin resistance in human ovarian cancer cells by maintaining endoplasmic reticulum and mitochondrial homeostasis. Oncol Rep. 2015;34:3051–60. https://doi.org/10.3892/or.2015.4283.
45. Xue J, Li R, Zhao X, Ma C, Lv X, Liu L, Liu P. Morusin induces paraptosis-like cell death through mitochondrial calcium overload and dysfunction in epithelial ovarian cancer. Chemico-Biol Interact. 2018;283:59–74. https://doi.org/10.1016/j.cbi.2018.02.003.
46. Zhao Y, Wang P, Liu T, Yang Y, Guo J, He Y, Xi J. Zn2 + protect cardiac H9c2 cells from endoplasmic reticulum stress by preventing mPTP opening through MCU. Cell Signal. 2022;100:110467. https://doi.org/10.1016/j.cellsig.2022.110467.
47. Zheng H-C. The molecular mechanisms of chemoresistance in cancers. Oncotarget. 2017;8:59950–64. https://doi.org/10.18632/oncotarget.19048.

Figures

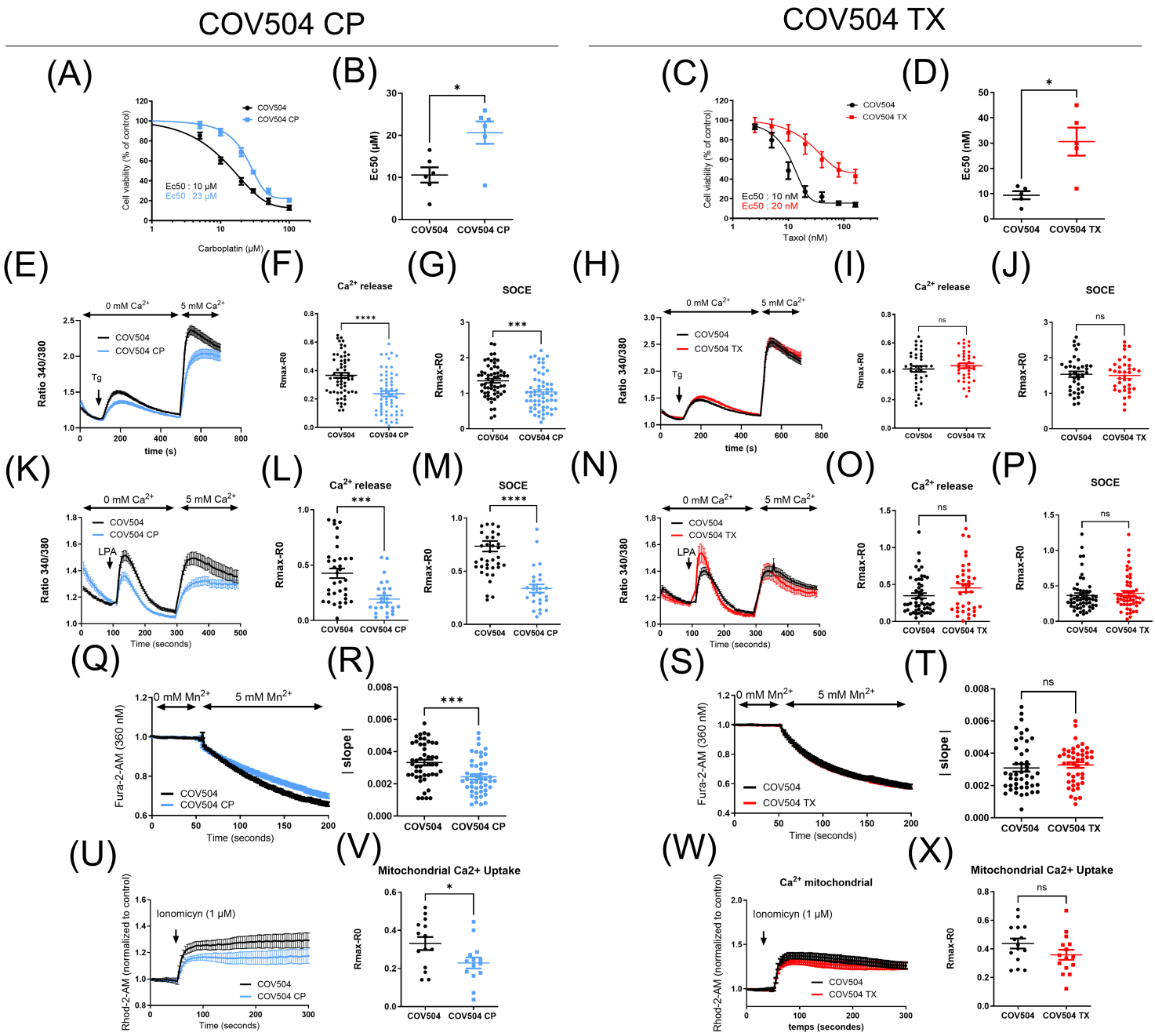


Figure 1

General dampening of Ca2+ signaling in COV504 CP, but not in COV504 TX. A, C. COV504, COV504 CP and COV504 TX cells were exposed to increasing concentrations of carboplatin (A, n=6) or Taxol® (C, n=5) in a 7-day survival assay. B, D. EC50 quantification from A and C. E, H. Fura-2 fluorescence traces showing cytosolic Ca^{2+} responses in COV504/COV504 CP (E) and COV504/COV504 TX (H). ER Ca^{2+} depletion was induced with 4 µM thapsigargin in Ca^{2+}-free PSS, followed by 5 mM Ca^{2+} re-addition to measure SOCE. Traces represent mean ± SEM: COV504 n=61, COV504 CP n=60 (E); COV504 n=38, COV504 TX n=37 (H). F, I. ER Ca^{2+} store depletion; G, J. maximal SOCE amplitude. K, N. Fura-2 traces following 10 µM lysophosphatidic acid (LPA) in Ca^{2+}-free PSS and subsequent 5 mM Ca^{2+} re-addition.

Mean ± SEM: COV504 n=35, COV504 CP n=26 (K); COV504 n=52, COV504 TX n=37 (N). L, O. ER Ca^{2+} store depletion; M, P. maximal SOCE amplitude. Q, S. Fura-2 traces measuring constitutive Ca^{2+} entry following 5 mM Mn^{2+} injection: COV504 n=47, COV504 CP n=47 (Q); COV504 n=45, COV504 TX n=45 (S). R, T. Constitutive Ca^{2+} entry quantified as the absolute slope. U, W. Rhod-2 traces measuring mitochondrial Ca^{2+} uptake induced by 1 µM ionomycin in 2Ca PSS: COV504 n=14, COV504 CP n=14 (U); COV504 n=15, COV504 TX n=15 (W). V, X. Quantification of mitochondrial Ca^{2+} uptake. Data are mean ± SEM from ≥4 independent experiments. Comparisons between COV504 and resistant cells were performed using the Mann-Whitney test: *p<0.05, **p<0.01, ***p<0.001.

Alt text: Analysis of plasma membrane and mitochondrial Ca^{2+} pathway in carboplatin or Taxol®-resistant high grade serous ovarian cancer cells.

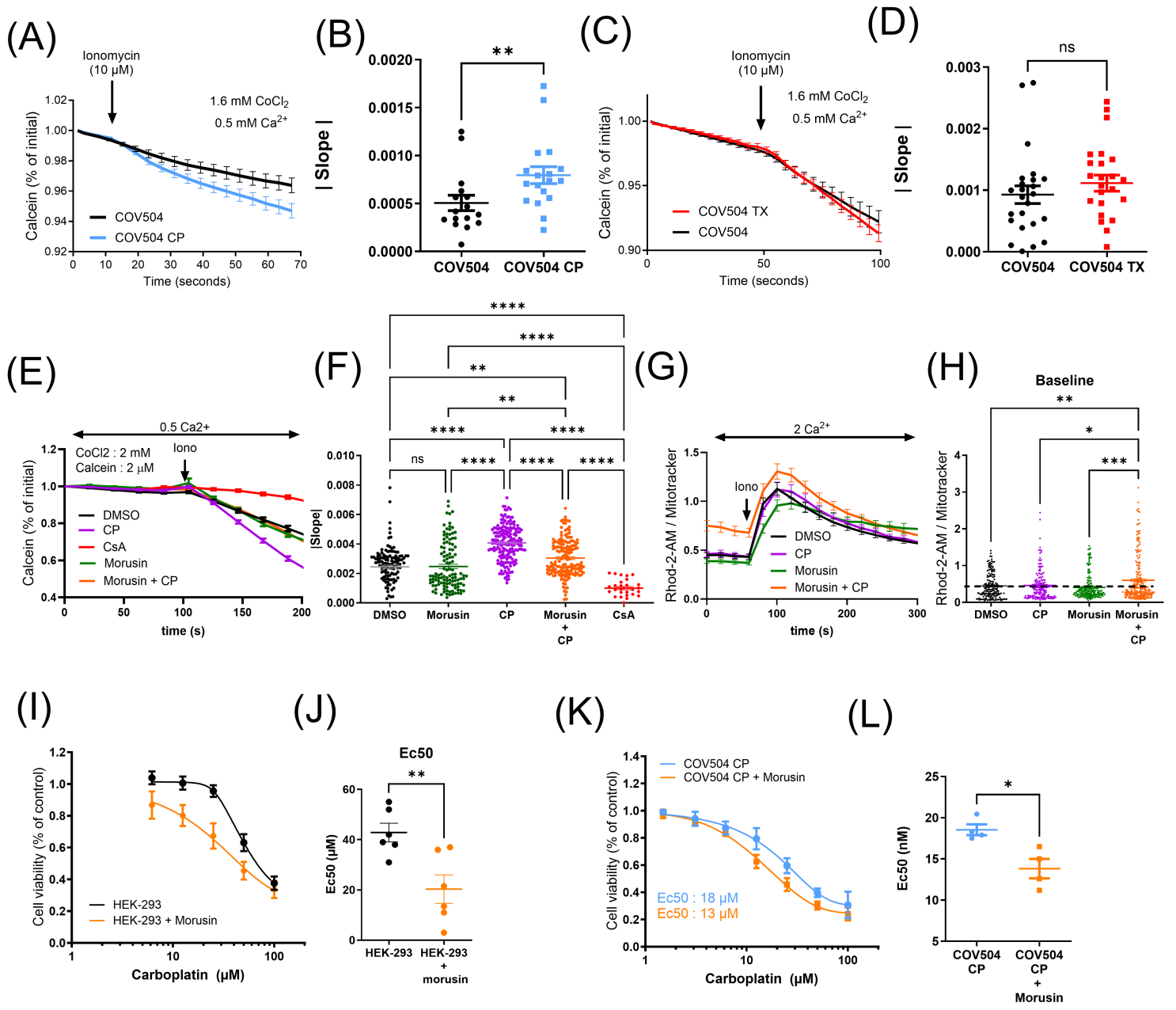


Figure 2

Carboplatin-induced mPTP hypersensitivity limits mitochondrial Ca2+ overload, and its pharmacological reversal by morusin potentiates carboplatin cytotoxicity. A, C. mPTP opening sensitivity measured using the CoCl2 method in COV504/COV504 CP (A, n=16/18) and COV504/COV504 TX (C, n=24/24). mPTP opening was induced with 10 µM ionomycin. B, D. Quantification of the immediate post-ionomycin slope from A and C, expressed as absolute values. E. mPTP opening sensitivity in HEK-293 cells treated for 24 h with DMSO, carboplatin (CP, 50 µM), morusin (1 µM) or CP + morusin. Ionomycin (10 µM) induced mPTP opening. n=122 (DMSO), 180 (CP), 115 (morusin), 159 (CP + morusin); cyclosporin A (CsA, 10 µM, n=28) was used as an mPTP inhibitor. F. Quantification of the immediate post-ionomycin slope from E. G. Rhod-2 traces showing mitochondrial Ca^{2+} responses in HEK-293 cells after 24 h treatment with DMSO, CP (50 µM), morusin (1 µM) or CP + morusin. H. Quantification of basal Rhod-2 fluorescence. Mean ± SEM: DMSO n=161, CP n=170, morusin n=186, CP + morusin n=226. I, J. HEK-293 cells were treated with increasing CP concentrations ± morusin (1 µM) in a 7-day survival assay (n=6); J, EC50 quantification. K, L. COV504 CP cells were similarly treated with increasing CP concentrations ± morusin (n=4); L, EC50 quantification. Data are mean ± SEM from ≥4 independent experiments. Statistical significance was assessed by Mann-Whitney or one-way ANOVA: *p<0.05, **p<0.01, ***p<0.001.

Alt text: Modulation of mPTP, mitochondrial Ca^{2+} and cell survival in carboplatin or Taxol®-resistant cells, as well as HEK-293.

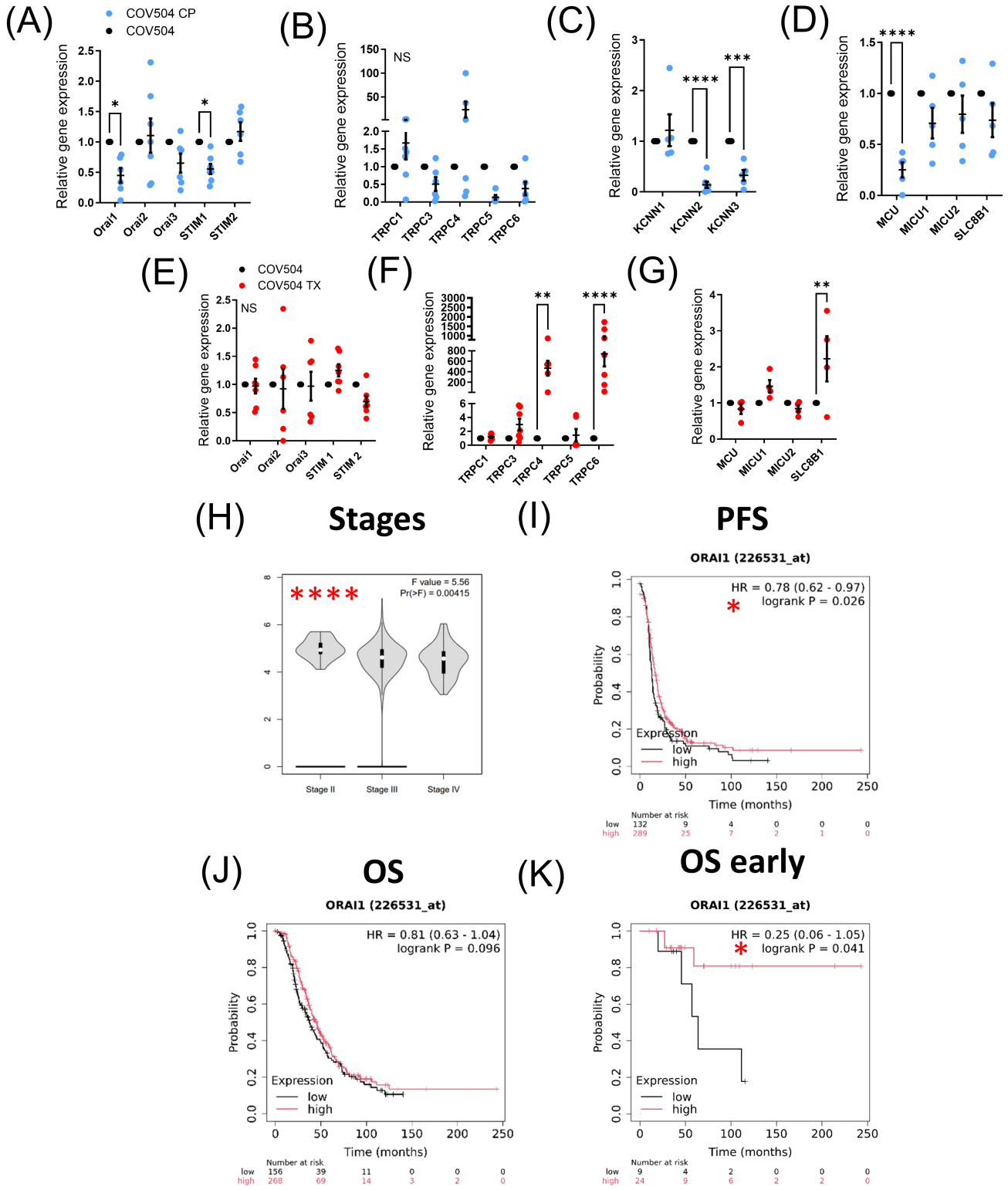


Figure 3

Lower expression of the Ca^{2+} signaling toolkit correlates with carboplatin resistance, while lower *Orai1* levels correlate with disease progression and shorter patient survival. A. SOCE machinery (*Orai1*, *Orai2*, *Orai3*, *STIM1*, *STIM2*) mRNA expression measured by qRT-PCR in COV504 and COV504 CP cells (n=7). B. TRPC channels (*TRPC1*, *TRPC3*, *TRPC4*, *TRPC5*, *TRPC6*) mRNA expression in COV504 and COV504 CP cells (n=7). C. SKCa channels (*KCNN1*, *KCNN2*, *KCNN3*) mRNA expression in COV504 and COV504 CP

cells (n=7). D. Mitochondrial Ca^{2+} toolkit (*MCU, MICU1, MICU2, SLC8B1*) mRNA expression in COV504 and COV504 CP cells (n=7). E. SOCE machinery mRNA expression in COV504 and COV504 TX cells (*Orai1, Orai2, Orai3, STIM1, STIM2*; n=7). F. TRPC channel mRNA expression (*TRPC1, TRPC3, TRPC4, TRPC5, TRPC6*; n=7) in COV504 and COV504 TX cells. G. Mitochondrial Ca^{2+} toolkit mRNA expression (*MCU, MICU1, MICU2, SLC8B1*; n=4) in COV504 and COV504 TX cells. H. *Orai1* mRNA expression across ovarian cancer stages analyzed using GEPIA. I–K. Kaplan-Meier analysis of progression-free survival (PFS; I), overall survival (OS; J), and OS in early-stage disease (stages 1+2; K) in patients with serous ovarian cancer treated with platinum-based therapy, stratified by *Orai1* mRNA expression using KMplotter. Data are mean ± SEM. Comparisons between COV504 and COV504 CP or COV504 TX cells were performed using the Mann-Whitney test: *p<0.05, **p<0.01, ***p<0.001. Kaplan-Meier survival analyses were performed using the log-rank test and reported as hazard ratios (HR) with confidence intervals (CI).

Alt text: mRNA expression of Ca^{2+} channels in carboplatin or Taxol®-resistant high grade serous ovarian cancer, followed by *Orai1* clinical relevance in ovarian cancer progression.

Supplementary Files

This is a list of supplementary files associated with this preprint. Click to download.

- DataaccessibilityRomitoOmPTP.xlsx